tion with Lipo-PGE_1. Specifically, there is no differences between generic formulations and innovator formulations in terms of PGE_1 retention rate in lipid particles. Thus the clinical effect of generic formulations will not differ greatly from that of innovator formulations.

References

Becher, P., 1957. Emulsions: Theory and Practice. Reinhold, New York, pp. 189–196.

Driscoll, D.F., Etzler, F., Barber, T.A., Nehne, J., Niemann, W., Bistrian, B.R., 2001. Physicochemical assessments of parenteral lipid emulsions: light obscuration versus laser diffraction. Int. J. Pharm. 219, 21–37.

Goto, N., Sakaya, H., Nakamura, T., Wakiya, Y., Masada, M., 2005. The 125th Annual Meeting of the Pharmaceutical Society of Japan 29-0816.

Golub, M., Zia, P., Matsuno, M., Horton, R., 1975. Metabolism of prostaglandins A1 and E1 in man. J. Clin. Invest. 56, 1404–1410.

Griffin, W.C., 1954. J. Soc. Cosmet. Chem. 5, 249.

Guyton, A.C., 1991. The microcirculation and the lymphatic system: capillary fluid exchange, interstitial fluid and lymph flow. In: Guyton, A.C. (Ed.), Textbook of Medical Physiology, 8th edn. Saunders, Philadelphia, pp. 170–184.

Igarashi, R., Nakagawa, M., Mizushima, Y., 1988. The bioactivity of esterified PGE1 and its application for lipid microspheres. Jpn. J. Inflamm. 8, 243–246.

Kramer, H.H., Sommer, M., Rammos, S., Krogmann, O., 1995. Evaluation of low dose prostaglandin E1 treatment for ductus dependent congenital heart disease. Eur. J. Pediatr. 154, 700–707.

Makita, S., Nakamura, M., Ohhira, A., Itoh, S., Hiramori, K., 1997. Effects of prostaglandin E1 infusion on limb hemodynamics and vasodilatory response in patients with arteriosclerosis obliterans. Cardiovasc. Drugs Ther. 11, 441–448.

Milio, G., Cospite, V., Cospite, M., 2003. Effects of PGE-1 in patients suffering from peripheral arterial occlusive disease. Minerva Cardioangiol. 51, 311–316.

Mizushima, Y., Hamano, T., Haramoto, S., Kiyokawa, S., Yanagawa, A., Nakura, K., Shintome, M., Watanabe, M., 1990. Distribution of lipid microspheres incorporating prostaglandin E1 to vascular lesions. Prostag. Leukot. Essent. Fatty Acids 41, 269–272.

Mizushima, Y., Yanagawa, A., Hoshi, K., 1983. Prostaglandin E1 is more effective, when incorporated in lipid microspheres, for treatment of peripheral vascular diseases in man.J Pharm. Pharmacol. 35, 666–667.

Otomo, S., Mizushima, T., Aihara, H., Yokoyama, K., Watanabe, M., Yanagawa, A., 1985. Prostaglandin E1 incorporated in lipid microspheres (Lipo PGE1). Drugs Exp. Clin. Res. 11, 627–631.

Sakaya, H., Goto, N., Nakamura, T., Wakiya, Y., Masada, M., 2005. The 125th annual meeting of the pharmaceutical society of Japan, 29-0815.

Schramek, P., Waldhauser, M., 1989. Dose-dependent effect and side-effect of prostaglandin E1 in erectile dysfunction. Br. J. Clin. Pharmacol. 28, 567–571.

Takenaga, M., Ohta, Y., Tokura, Y., Hamaguchi, A., Igarashi, R., 2007. Comparison study of lipo PGE1 preparations. Yakugaku Zasshi 127, 1237–1243.

Teagarden, D.L., Anderson, B.D., Petre, W.J., 1988. Determination of the pH-dependent phase distribution of prostaglandin E1 in a lipid emulsion by ultrafiltration. Pharm Res. 5, 482–487.

Yamaguchi, T., Fukushima, Y., Itai, S., Hayashi, H., 1995. Rate of release and retentivity of prostaglandin E1 in lipid emulsion. Biochim. Biophys. Acta 1256, 381–386.

Washington, C., Chawla, A., Christy, N., Davis, S.S., 1989. The electrokinetics properties of phospholipid-stabilized fat emulsions. Int. J. Pharm. 54, 191–197.

Washington, C., 1990. The stability of intravenous fat emulsions in total parenteral-nutrition mixtures. Int. J. Pharm. 66, 1–21.

Division of Drugs[1], National Institute of Health Sciences, Tokyo, Japan; TeraView Limited[2], St John's Innovation Park, Cambridge, United Kingdom; TDDS Research Laboratory[3], Hisamitsu Pharmaceutical Co. Inc., Tsukuba; Bruker Optics K.K[4], Tokyo, Japan

Detection of tulobuterol crystal in transdermal patches using Terahertz pulsed spectroscopy and imaging

T. Sakamoto[1], A. Portieri[2], P. F. Taday[2], Y. Takada[3], D. Sasakura[4], K. Aida[3], T. Matsubara[4], T. Miura[4], T. Terahara[3], D. D. Arnone[2], T. Kawanishi[1], Y. Hiyama[1]

Received January 19, 2009, accepted February 21, 2009

Dr. Tamoaki Sakamoto, Division of Drugs, National Institute of Health Sciences, 1-18-1, Kami-yoga, Setagaya-ku, Tokyo 158-8501, Japan
tsakamot@nihs.go.jp

Pharmazie 64: 361–365 (2009) *doi: 10.1691/ph.2009.9022*

Applicability of a Terahertz Pulsed Spectroscopy (TPS) and a Terahertz Pulsed Imaging (TPI) for detection of tulobuterol (TBR) crystals in transdermal patches was investigated. Because TBR has high permeability in dermis, crystalline TBR in patch matrices contributes to controlling the release rate of TBR from a matrix. Therefore, crystalline TBR is one of the important factors for quality control of TBR transdermal tapes. A model tape that includes 5 w/w%, 10 w/w%, 20 w/w% or 30 w/w% of TBR was measured by TPS/TPI. TBR crystals in the matrices were successfully detected by TPI. Identification of TBR in an image of a crystal-like mass was done by comparison between the spectra of tapes and a TBR standard substance. These results indicate that TPS and TPI are applicable to identifying crystalline lumps of an active drug in tapes for quality control.

1. Introduction

Terahertz (THz) time-domain spectroscopy gives an electric field record of time delay due to the presence of material in a beam path with a higher refractive index when compared to a reference. Fourier-transformed waveforms from an electric field show a characteristic relationship between frequency and absorbance. Fourier-transformed waveforms provide information about not only intra-molecular vibration and lattice vibration, but also intermolecular forces and hydrogen bonds.

In the pharmaceutical industry, applications of TPS and TPI for discrimination of polymorphs (Taday et al. 2003; Walther et al. 2003; Strachan et al. 2004, 2005; Zeitler et al. 2005, 2006, 2007, Day et al. 2006) and for detecting unique waveforms of APIs have been reported. Thus, these technologies are expected to be used for qualitative and/or quantitative analysis (Taday et al. 2003; Upadhya et al. 2003; Ueno et al. 2006; Zeitler et al. 2006). In particular, THz spectroscopy has been used for detecting foreign materials in samples and for measuring the thickness of coatings (Fitzgerald et al. 2005; Zeitler et al. 2006; Ho et al. 2007).

Tulobuterol ((*R,S*)-2-tert-butylamino-1-(2-chlorophenyl) ethanol, TBR) transdermal tapes are used to cure bronchial asthma as a bronchodilator (β_2-blocker). TBR is one of the suitable compounds for systemic transdermal formulation because it has very high permeability into the keratin layer. The release rate of TBR from the matrix is controlled by the formation of lumps of TBR crystals. For this reason, crystallization of TBR in a matrix is an important factor assuring the quality of this tape. However, verifying the crystallization of an active drug is difficult because TDDS tapes (or patches) generally have a sandwich-like structure with a matrix between a liner and a supporting board. Although release testing is often used to evaluate "releasability", which is one of the physico-chemical properties of an active drug in transdermal pharmaceuticals, releasability is not a suitable parameter for evaluating crystallization of an active drug. In order to compensate for this disadvantage, development of an alternative method by which to observe crystallization of an active drug in a matrix through a liner and/or a supporting board is needed. This manuscript describes the applicability of one of the innovative non-destructive analytical techniques, TPS and TPI, for quality evaluation of TDDS tapes.

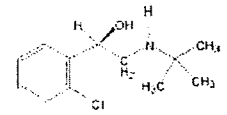

Tulobuterol

2. Investigations, results and discussions

2.1. THz pulsed spectrum of TBR obtained by TPS instrument

Fig. 1(A) shows the typical THz electric field records obtained from the TBR pellet and reference (PE pellet) by

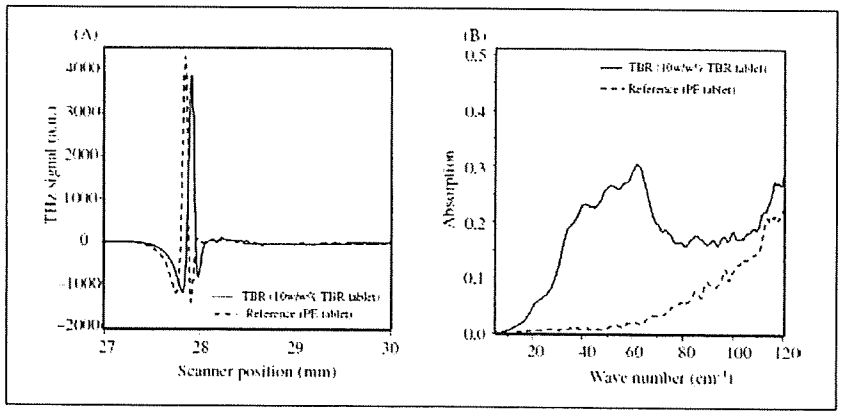

Fig. 1:
THz electric field records (A) and Fourier-transformed THz waveforms (B) of the TBR pellet and reference (PE pellet). The unique absorbance range, from 40 cm^{-1} to 70 cm^{-1}, is available to detect TBR absorbance

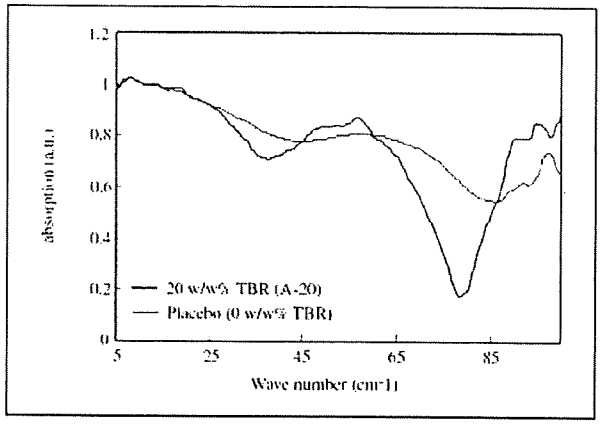

Fig. 2: THz spectra of model tape (20 w/w%, A-20) and placebo tape (0 w/w% TBR) obtained with quartz. The characteristic THz spectral range of TBR (from 45 cm^{-1} to 70 cm^{-1}) is best observed when etaloning effects are not dominating the range due to the thinness of the sample, as was the case here

the TPS 1000. The THz electric field record of the TBR pellet was shifted compared with that of the reference and the unique Fourier-transformed THz waveform of TBR was observed compared with that of the PE reference (Fig. 1(B)). This unique absorbance range, from 70 cm^{-1} to 45 cm^{-1}, seemed to be available to detect TBR absorbance from the total waveform of tapes.

2.2. *THz image and spectra of TBR crystal in matrix*

Fig. 2 shows the Fourier-transformed THz spectra of the placebo tape (the red line, an acrylic matrix) and the model tape (the blue line, 20w/w% TBR in an acrylic matrix, A-20). The fingerprint-like waveform of TBR from 70 cm^{-1} to 45 cm^{-1} was observed in the THz spectra obtained from the A-20. This observation suggests that chemical information of TBR can be detected in a tape. A lump of TBR crystals was detected at the top left of the image (Fig. 3(A)). The TPI contrast derives from refractive index differences. Therefore, it was presumed that the edge of the lumps of the TBR crystals contributed to making the definite contrast of shift of the refractive index. However, the image that is made from the shift of a refractive index would not provide chemical information about the lumps of TBR crystals. In order to identify the origin of the lumps of crystals, the THz spectra obtained from pixels which are located inside the lumps or outside the lumps were compared. Both spectra are shown in Fig. 3(B). The waveform indicated as the blue line represents the THz spectrum obtained from the pixel that is located inside the lump of crystals. The red line indicates the spectrum obtained from a pixel that is located outside the lump of crystals. The THz spectrum from the crystal shows a characteristic waveform range from 70 cm^{-1} to 45 cm^{-1}, almost the same as that of TBR standard substance. This observation strongly suggests that an image could be obtained from the crystal formed from TBR.

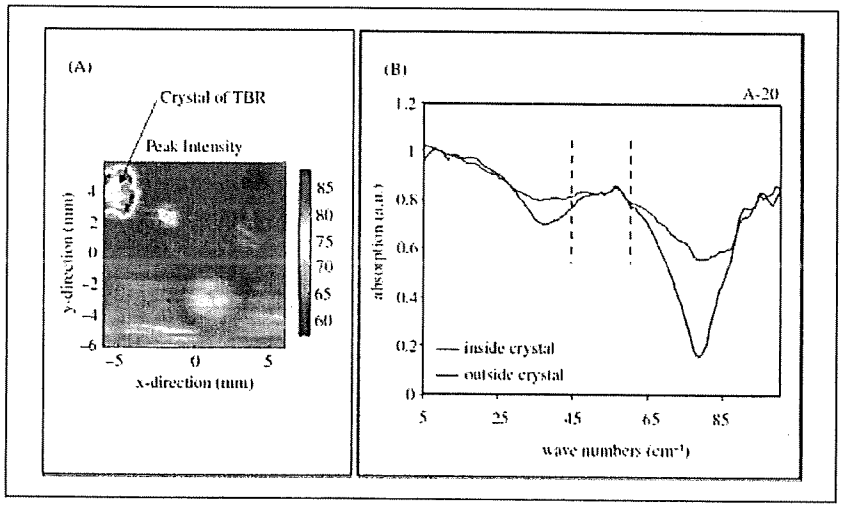

Fig. 3:
THz image of TBR crystal (A) and Fourier-transformed waveforms of pixels inside and outside of the crystals (B), obtained from A-20. The aggregation of TBR crystals which the arrow points to was clearly identified (A). It should be possible to observe the characteristic spectrum of TBR (from 45 cm^{-1} to 60 cm^{-1}) from both pixels located inside and outside of the crystal, but etaloning effects are again dominating the spectra

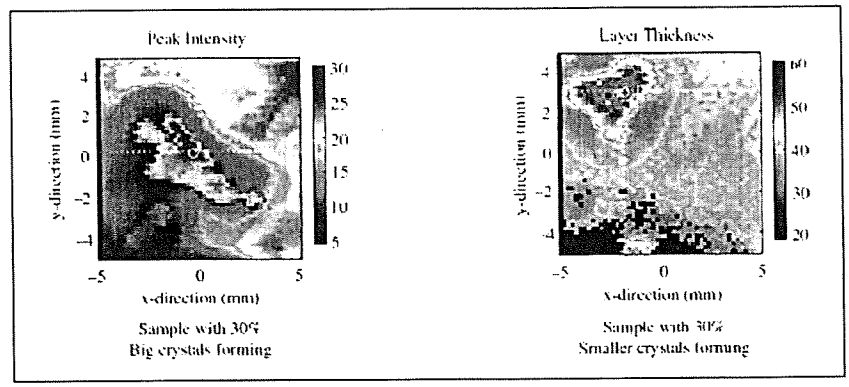

Fig. 4:
THz image of TBR crystals in matrix obtained using TPI 1000. Several sizes of TBR crystals were detected in the scanned area (the longer diameters: 0.5 mm to 3 mm, the shorter diameters: 0.1 mm to 0.2 mm)

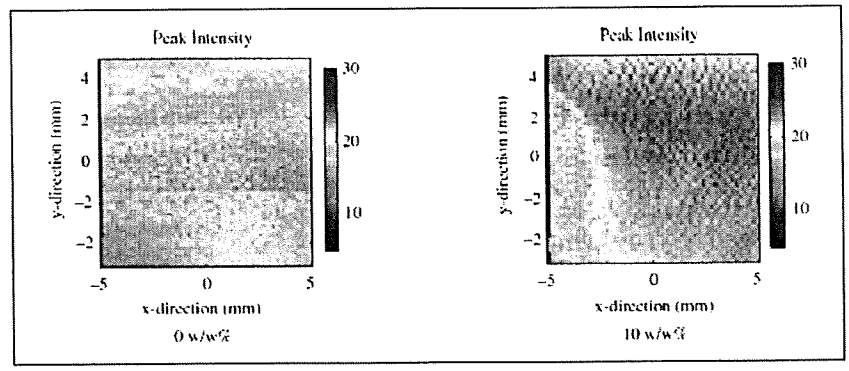

Fig. 5:
THz images of model tapes (0 and 10 w/w% TBR). Although there should be many small white crystals in R-10, only some were detected in the scanned area. In cases where the white crystals cannot be observed, the crystals might be smaller than the spatial resolution (100 μm) of TPI. Further studies need to be carried out to investigate differences in the samples

2.3. Size of crystals and spatial resolution of TPI

Fig. 4 shows the THz image obtained from the model tape (30 w/w% TBR, an acrylic matrix, A-30). Both model tapes were obtained from the same batch. Several sizes (short: 0.1 mm–0.2 mm, long: 0.5 mm–3 mm) of crystals were observed in these images.

The THz images obtained from the placebo tape (a rubber matrix, R-0) and the model tape (10 w/w% TBR, rubber matrix, R-10) are shown in Fig. 5. The image on the right side was obtained from R-10. Although small white crystals can be observed through a liner or a supporting board, no image of the lumps was observed in the THz image. This suggested that the sizes of the TBR crystals were smaller than the spatial resolution of TPI (approximately 100 μm). According to our study using Microscopic Laser Raman Spectroscopy/Mapping, the size of the TBR crystals was estimated to be from 6 μm to 40 μm (Sakamoto et al. 2006, 2007).

2.4. Depth image of crystals in TDDS tape

The THz image of A-30 and its depth image are shown in Fig. 6. The thickness of the lump of crystals in the matrix increased. The refractive index of the THz pulse was shifted due to the edges of the lumps of TBR crystals. This suggested that a comparatively big shift of a refractive index provides a definite image.

In conclusion, it was shown that THz spectroscopy/imaging technology was useful for detecting lumps of crystals of an active drug in transdermal tapes. THz spectroscopy/imaging can provide unique physical (and/or certain kinds of chemical) information compared with near infrared and/or mid infrared spectroscopy/imaging. In particular, obtaining a depth image from a pharmaceutical sample would be very useful for gaining an in-depth understanding of the quality of pharmaceuticals.

Although approximately 100 μm of spatial resolution in the THz pulsed image would hinder the detection of min-

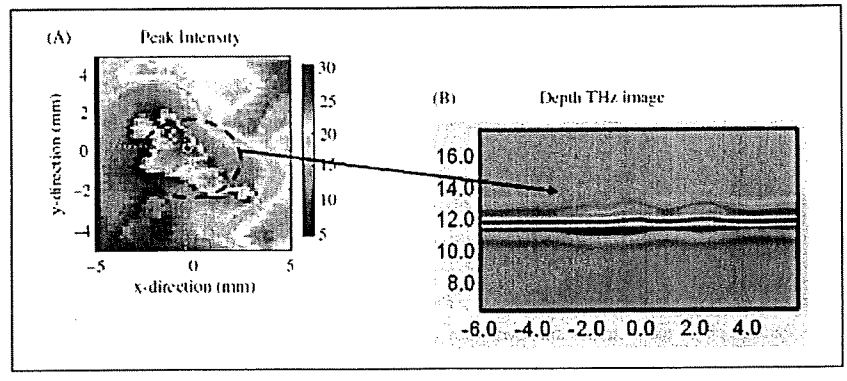

Fig. 6:
THz image of TBR crystal and depth THz image of matrix (A). The depth THz image in the scanned area where the crystal is observed shows the change in the thickness of the tape that can be seen (B)

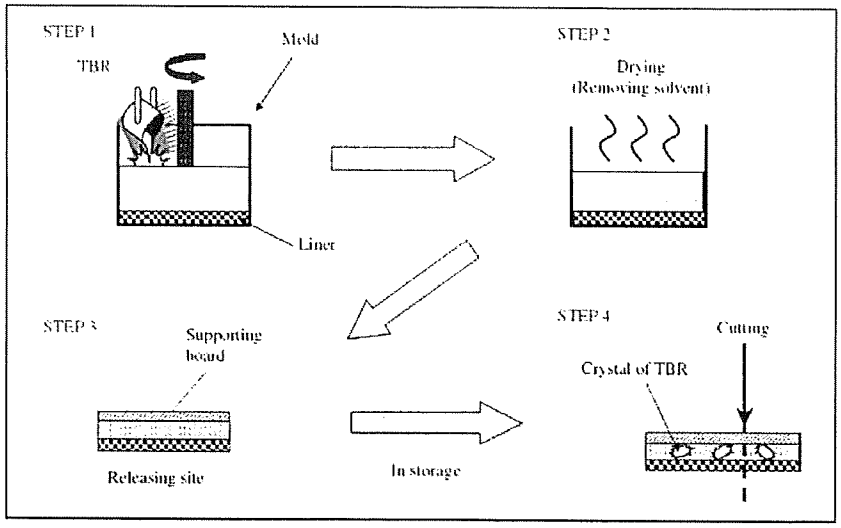

Fig. 7:
Flowchart showing preparation of model tapes. Residual solvents were removed by heating, and the mold was used to produce a sheet of model tape with a constant thickness and area

ute particles that are smaller than the spatial resolution, a reflective index of the THz pulsed wave may provide other useful information. Moreover, it would be able to detect problems caused by the manufacturing process, such as mixing of air bubbles and heterogeneity of active substances in the matrix. Therefore, this technology would be useful as an analytical tool not only for pharmaceutical quality control, but also for process control in pharmaceutical manufacturing.

Table: Prepared model transdermal tapes in this study

TBR level	Acrylic matrix	Rubber matrix
0 w/w% (Placebo)	A-0	R-0
10 w/w%	–	R-10
20 w/w%	A-20	–
30 w/w%	A-30	–

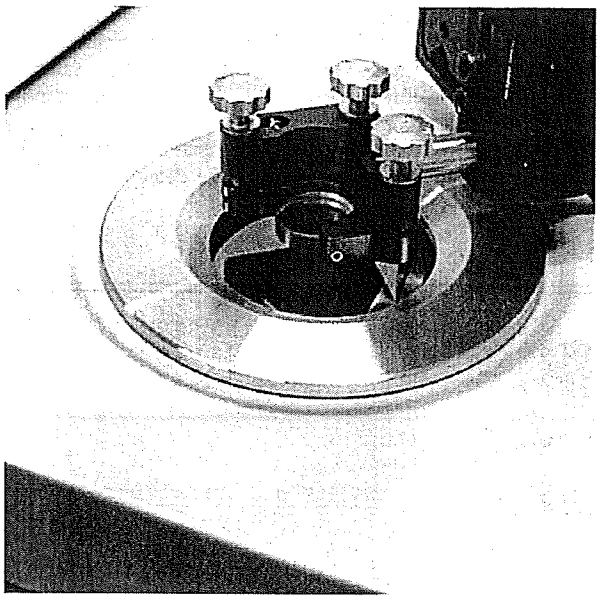

Fig. 8: Photograph of the metallic arm used when measuring the sample with a reference mirror

3. Experimental

3.1. Materials

TBR (purity > 99.0%) and model tapes were supplied by Hisamitsu Pharmaceutical Co Inc (Tokyo, Japan). Polyethylene (PE) powder of particle size < 80 μm was supplied by Induchem.

3.2. Model tapes

The model tapes were prepared by TDDS Laboratory, Hisamitsu Pharmaceutical Co Inc (Tsukuba, Japan). In order to identify crystals of TBR in the matrix, two kinds of matrices, rubber and acrylic matrices, were prepared. The flowchart for preparing the model tapes is shown in Fig. 7. TBR and other ingredients of the adhesive solutions were stirred in the mold adequately. The mixture was extended on the liner and residual solvents were removed by drying. When the thickness of the matrix (the adhesive layer) became a constant (approximately 50 μm thickness), a supporting board was pasted on the matrix after removing the mold. A polyethylene terephthalate (PET) film was selected as a liner and as a supporting board, for both the model and the placebo tape. And then these tapes cut to a size of 36 mm diameter. TBR crystals in model tapes were generated by leaving the tapes to crystallize for some time.
The model tape that contained 0 w/w% (R-0, placebo), 5 w/w% (R-5) or 10 w/w% (R-10) of TBR in a rubber matrix consisted of polyisobutylene, polybutene and lipocyclic petroleum resin. Small white crystals were seen in all areas of the matrix in the A-10 through a liner or a supporting board. The model tape that contained 0 w/w% (A-0, placebo), 20 w/w% (A-20) or 30 w/w% (A-30) of TBR in an acrylic matrix consisted of acryl adhesion polymer and isopropyl myristate. On the A-30 samples, small white crystals were seen in all areas of the matrices. A higher TBR concentration was needed to generate the crystals in the acrylic matrix compared with the rubber matrix because of the solubility of TBR. The prepared model tapes are shown in the Table.

3.3. Apparatus and measurements

3.3.1. Transmittance measurement of tablet by TPS

In order to identify a THz spectrum of TBR, a pellet containing approximately 10 w/w% of TBR was prepared by compressing at 2 t for 3 min with a press machine. The pellet was measured using a TPS 1000 spectrometer (TeraView Limited, Cambridge, UK). Each sample was measured covering the spectral range from 120 cm^{-1} to 2 cm^{-1} at 1.5 cm^{-1} of spectral resolution. Spectra were obtained averaging 1800 scans.

3.3.2. Transmittance-reflectance measurements of tapes by TPI

A reference mirror was first measured, and then the samples were mounted to the mirror and adjusted horizontally against the measurement window of the TPI Imaga™ 1000 instrument (Fig. 8); subsequently, THz radiation was focused onto the samples to gain maximum sensitivity. Placebo tapes were used as a background for all measurements.
A TPI imaging system, TPI Imaga 1000 (TeraView Ltd., Cambridge, UK), was used for the reflectance measurement, which was operated in the rapid scan mode. Terahertz images were obtained by raster scanning the terahertz beam across the sample, which was mounted at the focus position. The scanned area was 12 mm × 12 mm, which corresponds to 120 pixels × 120 pixels at 100 μm spatial resolution. The total measurement time was approximately 30 min.

Acknowledgement: This study was supported in part by a research grant from the Ministry of Health, Labour and Welfare of Japan (H17-iyaku-ippan-040).

References

Day GM, Zeitler JA, Jones W, Rades T, Taday PF (2006) Understanding the influence of polymorphism on phonon spectra: Lattice dynamics calculations and terahertz spectroscopy of carbamazepine. J Phys Chem B 110: 447–456.

Fitzgerald AJ, Cole BE, Taday PF (2005) Nondestructive analysis of tablet coating thicknesses using terahertz pulsed imaging. J Pharm Sci 94: 177–183.

Ho L, Müller R, Römer M, Gordon KC, Heinämäki J, Kleinebudde P, Pepper M, Rades T, Shen YC, Strachan CJ, Taday PF, Zeitler JA (2007) Analysis of sustained-release tablet film coats using terahertz pulsed imaging. J Control Release 119: 253–261.

Sakamoto T, Fujimaki Y, Hiyama Y (2007) Study on development of quality analytical method using spectroscopic and imaging technique I. Application of Raman spectroscopy and mapping microscopy for quality evaluation of TDDS and Granules formulations. PharmTech Japan 23: 27–36 (in Japanese).

Sakamoto T, Matsubara T, Sasakura D, Takada Y, Fujimaki Y, Aida K, Miura T, Terahara T, Higo N, Kawanishi T, Hiyama Y (2009) Chemical mapping of tulobuterol in transdermal tapes using Microscopic Laser Raman Spectroscopy. Pharmazie 64: 166–171.

Strachan CJ, Taday PF, Newnham DA, Gordon KC, Zeitler JA, Pepper M, Rades T (2005) Using terahertz pulsed spectroscopy to quantify pharmaceutical polymorphism and crystallinity. J Pharm Sci 94: 837–846.

Strachan CJ, Rides T, Newnham DA, Gordon KC, Pepper M, Taday PF (2004) Using terahertz pulsed spectroscopy to study crystallinity of pharmaceutical materials. Chem Phys Lett 390: 20–24.

Taday PF, Bradley IV, Arnone DD, Pepper M (2003) Using terahertz pulse spectroscopy to study the crystalline structure of a drug: a case study of the polymorphs of ranitidine hydrochloride. J Pharm Sci 92: 831–838.

Ueno Y, Rungsawang R, Tomita I, Ajito K (2006) Quantitative measurements of amino acids by terahertz time-domain transmission spectroscopy. Anal Chem 78: 5424–5428.

Upadhya PC, Shen YC, Davies AG, Linfield EH (2003) Terahertz time-domain spectroscopy of glucose and uric acid. J Biol Phys 29: 117–121.

Walther M, Fischer BM, Jepsen PU (2003) Noncovalent intermolecular forces in polycrystalline and amorphous saccharides in the far infrared. Chem Phys 288: 261–268.

Zeitler JA, Newnham DA, Taday PF, Strachan CJ, Pepper M, Gordon KC, Rades T (2005) Temperature dependent terahertz pulsed spectroscopy of carbamazepine. Thermochim Acta 436: 70–76.

Zeitler JA, Shen YC, Baker C, Taday PF, Pepper M, Rades T (2006) Analysis of coating structure and interfaces in solid oral dosage forms by three dimensional terahertz pulsed imaging. J Pharm Sci 96: 330–340.

Zeitler JA, Newnham DA, Taday PF, Threlfall TL, Lancaster RW, Berg RW, Strachan CJ, Pepper M, Gordon KC, Rades T (2006) Characterization of temperature-induced phase transitions in the five polymorphic forms of sulfathiazole by terahertz pulsed spectroscopy and differential scanning calorimetry. J Pharm Sci 95: 2486–2498.

Zeitler JA, Taday PF, Pepper M, Rades T (2007) Relaxation and crystallization of amorphous carbamazepine studied by terahertz pulsed spectroscopy. J Pharm Sci 96: 2703–2709.

Stabilization of Protein Structure in Freeze-Dried Amorphous Organic Acid Buffer Salts

Ken-ichi IZUTSU,*[,a] Saori KADOYA,[b] Chikako YOMOTA,[a] Toru KAWANISHI,[a] Etsuo YONEMOCHI,[b] and Katsuhide TERADA[b]

[a] *National Institute of Health Sciences; 1–18–1 Kamiyoga, Setagaya-ku, Tokyo 158–8501, Japan: and* [b] *Faculty of Pharmaceutical Sciences, Toho University; 2–2–1 Miyama, Funabashi, Chiba 274–8510, Japan.*
Received May 6, 2009; accepted August 5, 2009; published online August 6, 2009

The purpose of this study was to elucidate the physical properties and protein-stabilizing effects of some pH-adjusting excipients (carboxylic acids and their sodium salts) in frozen solutions and in freeze-dried solids. Thermal and powder X-ray diffraction (XRD) analysis indicated a high propensity of sodium citrates to form glass-state amorphous solids upon freeze-drying. Some salts (*e.g.*, sodium succinate) crystallized in the single-solute frozen solutions. FT-IR analysis of bovine serum albumin (BSA) and bovine immunoglobulin G (IgG) in the aqueous solutions and the freeze-dried solids showed that some glass-forming salts (*e.g.*, monosodium citrate) protected the secondary structure from lyophilization-induced perturbation. Freeze-drying of BSA at different concentrations indicated retention of the secondary structure at similar monosodium citrate/protein concentration ratios, suggesting stabilization through direct interaction that substitute water molecules inevitable for the conformation integrity. The carboxylic acid salts should provide rigid hydrogen bonds and electrostatic interactions that raise the glass transition temperature of the amorphous solids and stabilize protein structure. The relevance of the structural stabilization to the protein formulation design was discussed.

Key words freeze-drying; protein formulation; stabilization; glass; Fourier transform infrared spectroscopy

The development of protein pharmaceuticals requires rational formulation design to ensure appropriate storage stability, because the degradation of such pharmaceuticals through various chemical and physical pathways not only reduces their therapeutic effects but also increases the risk of product immunogenicity.[1—5] Freeze-drying is a popular method of conferring long-term stability of therapeutic proteins that is not achievable in aqueous solutions. Removal of the surrounding water molecules during the freeze-drying process, however, often perturbs the protein structure, leading to irreversible aggregation in the reconstituted solutions. The structurally altered protein molecules are also prone to chemical degradation during storage.[1] Maintaining the protein conformation by process and ingredient (*e.g.*, stabilizer, pH buffer, isotonic agents) optimization thus improves both the physical and chemical stability of protein formulations.

Choosing the solution pH and buffer system appropriate to a particular protein is a simple but significant element in the formulation design because the chemical and physical integrity of proteins in the aqueous solutions and freeze-dried solids depend largely on the pH.[6] Some buffer components also favorably or adversely affect the protein stability through direct interactions and/or through changing the local environments in the dried state. For example, freezing of certain buffer systems (*e.g.*, sodium phosphate) often induces crystallization of a component salt and resulting shift of the local pH surrounding the proteins.[7—11] Freeze-drying from some buffer systems (*e.g.*, L-histidine, citrate, or Tris) often leads to higher activity retention of proteins (*e.g.*, coagulation factor VIII, recombinant human interleukin-1 receptor antagonist) relative to those from other buffers.[12—15] Conformation of the proteins lyophilized in these buffer systems is of particular interest.

Reported properties of some carboxylic acid salts, including stabilization of native protein conformation in aqueous solutions (*e.g.*, antithrombin III)[16,17] and their propensity to form glass-state amorphous solids upon lyophilization,[18] suggest their ability to protect protein conformation against dehydration stress through mechanisms similar to disaccharides. Non-reducing disaccharides (*e.g.*, sucrose, trehalose) are popular stabilizers in solution and freeze-dried protein formulations. Various saccharides and polyols thermodynamically favor native protein structures over denatured states in aqueous solutions by a "preferential exclusion" mechanism.[19] Sucrose and trehalose protect proteins by substituting surrounding water molecules through hydrogen bonds during the freeze-drying process.[4,20—22] Limited molecular mobility in glass-state lyophilized disaccharide solids also protects embedded proteins from chemical degradation (*e.g.*, deamidation) during storage.[23]

The present study assesses the physical properties and protein-stabilizing effects of carboxylic acid buffer systems (*e.g.*, sodium citrate, sodium L-tartrate, sodium succinate) and their constituting salts against lyophilization-induced protein secondary structure changes. The physical properties of the frozen solutions and freeze-dried solids were studied by powder X-ray diffraction and thermal analysis. The effects of carboxylic acids and their sodium salts on the structural integrity of model proteins rich in α-helices [bovine serum albumin (BSA)] or β-sheets [bovine immunoglobulin G (IgG)], both prior to and after the freeze-drying process, were studied by Fourier transform infrared (FT-IR) spectroscopy of the amide I band combined with a mathematical band-narrowing technique (second-derivative).[24] Possible mechanisms of structural stabilization and their implications for formulation design are discussed.

Experimental

Materials Bovine serum albumin (A-7511, fatty acid content: approximately 0.005%, pI: 4.9), dextran 10.2k, and bovine immunoglobulin G (#64140) were purchased from Sigma-Aldrich Co. (St. Louis, MO, U.S.A.) and ICN Biomedicals Inc. (Aurora, OH, U.S.A.), respectively. Disodium hydrogen citrate sesquihydrate, monosodium citrate, and disodium(+)-tartrate dihydrate were obtained from Kanto Chemical Co. (Tokyo, Japan). Sodium

* To whom correspondence should be addressed. e-mail: izutsu@nihs.go.jp

hydrogen L-tartrate was purchased from Alfa Aesar GmbH & Co KG (Karlsruhe, Germany). Citric acid monohydrate, trisodium citrate dihydrate, sodium hydrogen L-tartrate, and other chemicals were purchased from Wako Pure Chemical, Co. (Osaka, Japan). The proteins were dialyzed overnight against buffer solutions (20 mM sodium phosphate, sodium citrate, sodium L-tartrate, sodium succinate, pH 6.0) using cellulose tubing (MWCO 14,000, Viskase Co., Darien, IL,U.S.A.). The dialyzed protein solutions were centrifuged (1500×*g*) and filtered (0.45 μm PVDF, Millipore, Bedford, MA, U.S.A.) before the freeze-drying study. Precipitation during dialysis reduced the IgG concentrations to 15—20 mg/ml in the resulting solutions. Monosodium succinate solution was prepared by mixing equivalent amounts of succinic acid and disodium succinate.

Freeze-Drying Freeze-drying was performed using a Freezone-6 lyophilizer equipped with temperature-controlled trays (Labconco, Kansas City, MO, U.S.A.). Aqueous solutions containing protein (10, 50 mg/ml) and various concentrations of excipients in flat-bottom glass vials (300 μl, 13 mm diameter) were placed on the shelf of the freeze-drier at room temperature. Some of the samples also contained low concentrations (1.5—10 mM) of the corresponding buffer system salts that were originally in the dialyzed protein stock solutions. The shelf was cooled to −40 °C at 0.5 °C/min and then maintained at this temperature for 2 h before the primary drying process. The frozen solutions were dried under vacuum (21 mTorr), with the shelf temperature maintained at −40 °C for 15 h, −30 °C for 6 h, and 35 °C for 6 h. The shelf was heated at a rate of 0.2 °C/min between the drying steps. The vials were sealed with rubber closures under vacuum. A pH meter (D-51, Horiba Ltd., Kyoto, Japan) and an electrode (9669-10D) were used to measure the pH values of solutions containing protein (*e.g.*, BSA) and excipients. The pH values of other solutions were obtained using a pH meter (HM-60G, TOA-DKK Co., Tokyo).

Thermal Analysis Thermal analysis of frozen solutions and dried solids was carried out using a differential scanning calorimeter (Q-10, TA Instruments, New Castle, DE, U.S.A.) and software (Universal Analysis 2000, TA Instruments). Aliquots of aqueous solutions (10 μl) in aluminum cells were cooled from room temperature at 10 °C/min and then scanned from −70 °C at 5 °C/min. Freeze-dried solids (0.5—1 mg) in hermetic aluminum cells were subjected to thermal analysis from −30 °C at 5 °C/min under nitrogen gas flow. Maximum inflection points in the heat flow discontinuities were assigned as glass transitions of maximally freeze-concentrated phases in frozen solutions (T_g') and glass transitions of freeze-dried solids (T_g).

Powder X-Ray Diffraction (XRD) Analysis Powder X-ray diffraction patterns were obtained at room temperature using a Rint-Altima diffractometer (Rigaku, Tokyo, Japan) with Cu$K\alpha$ radiation at 40 kV/50 mA. The samples were scanned through the range $5° < 2\theta < 35°$ at an angle speed of 5 °/min.

Measurement of Residual Water The amount of water in the freeze-dried solids suspended in dehydrated methanol was determined by the Karl–Fischer method using an AQV-6 volumetric titrator (Hiranuma Sangyo, Ibaraki, Japan).

Fourier-Transform Infrared Spectroscopy (FT-IR) The secondary structures of proteins were analyzed using an FT-IR system (MB104 spectrophotometer (ABB Bomen, Quebec, Canada) with PROTA (Bomen/Vysis) and GRAMS/32 (Galactic Ind. Co.) software. Transmission spectra of freeze-dried proteins were obtained from 256 scans of pressed disks containing freeze-dried solids (approx. 1 mg protein) and potassium bromide (approx. 250 mg) at a resolution of 4 cm^{-1}. Spectra of aqueous protein solutions (10 mg/ml) were recorded from 512 scans using an infrared cell with CaF_2 windows and a film spacer (6 μm). Reference spectra were recorded with the corresponding buffer and excipient solutions to obtain the absorbance spectra using an automated subtraction algorithm in PROTA. The second-derivative spectra obtained with the Savitski–Golay derivative function (7-point smoothing) were baseline-corrected and area-normalized in the amide I region (1600—1715 cm^{-1}).[25,26]

Results

The physical properties of organic acids and their sodium salts are summarized in Table 1. Thermal analysis indicated varied propensities of the excipients to crystallize in the frozen solutions. Frozen monosodium L-tartrate solution showed two exotherm peaks that indicate eutectic crystallization. Pairs of exothermic and endothermic peaks indicated eutectic solute crystallization and subsequent melting in the frozen mono- and disodium succinate solutions. A flat thermogram in the heating scan suggested crystallization of succinic acid in the cooling process. Other frozen excipient solutions showed thermal transition of the freeze-concentrated non-ice phase at certain temperatures (T_g': glass transitions of maximally freeze-concentrated phases).[4,27] Physical properties of some frozen buffer solutions (50 mM, pH 6.0) reflected those of the constituent salts. Frozen sodium citrate and sodium L-tartrate buffer solutions showed T_g' at −41.6 and −39.7 °C, respectively. In contrast, eutectic crystallization of their constituent salts resulted in an exotherm peak (−28.8 °C) and an endotherm peak (−9.6 °C) in the frozen sodium succinate buffer. The addition of BSA (10 mg/ml) and accompanying small amount of the buffer components (1.5 mM, pH 6.0) reduced the pH variation of the aqueous excipient (50 mM) solutions. A higher transition temperature (T_g') and the eutectic crystallization temperatures suggested reduced mobility of solute molecules in the freeze-concentrated mixture with BSA.[8]

Figure 1 shows thermograms of freeze-dried excipient solids. Heating scans of cake-structure freeze-dried monosodium L-tartrate, succinic acid, and monosodium succinate solutions

Table 1. Physical Properties of Carboxylic Acid and Their Sodium Salts

Excipients[a]	Frozen solutions				Freeze-dried solids		
	w/o BSA		with 10 mg/ml BSA		with 10 mg/ml BSA		
	pH	Thermal property	pH	Thermal property	Crystallinity[b]	Thermal property	Residual water (%)
Na_3-citrate	8.51	T_g': −43.0±1.2 °C	7.06	T_g': −35.8±0.1 °C	Amorphous	T_g: 74.9±2.0 °C	5.2±0.9
Na_2H-citrate	5.28	T_g': −39.1±0.0 °C	5.30	T_g': −31.6±0.2 °C	Amorphous	T_g: 78.2±2.6 °C	5.1±0.9
NaH_2-citrate	3.72	T_g': −33.2±0.2 °C	3.97	T_g': −24.4±1.1 °C	Amorphous	T_g: 61.1±1.8 °C	5.2±0.0
Citric acid	2.29	T_g': −55.0±0.3 °C	2.63	n.d.	Amorphous	T_g: 43.7±1.8 °C	5.5±1.8
Na_2-L-tartrate	7.24	T_g': −40.0±0.1 °C	6.73	T_g': −32.6±0.1 °C	Amorphous	T_g: 68.8±2.6 °C	4.9±2.1
NaH-L-tartrate	3.50	Exotherm: −26.2, −15.0 °C	3.72	Exotherm: −10.9 °C	Amorphous	T_g: 56.6±3.8 °C	7.0±2.2
L-Tartric acid	2.26	T_g': −56.6±0.8 °C	2.56	n.d.	Amorphous	T_g: 43.7±1.8 °C	8.4±0.4
Na_2-succinate	8.00	Exotherm: −36.6 °C Endotherm: −7.8 °C	6.90	Exotherm: −21.3 °C Endotherm: −8.4, −6.0 °C	Amorphous	n.d.	5.3±1.1
NaH-succinate[c]	4.73	Exotherm: −25.0 °C Endotherm: −8.1 °C	4.81	T_g': −39.5±0.7 °C Endotherm: −7.9 °C	Amorphous	T_g: 49.2±3.7 °C	7.7±1.2
Succinic acid	2.82	Unclear	3.41	Exotherm: −17.6 °C	Amorphous	T_g: 42.0±6.2 °C	6.0±1.3

a) 50 mM. *b*) Obtained by powder X-ray diffractometry. *c*) Prepared by mixing and disodium succinate and succinic acid.

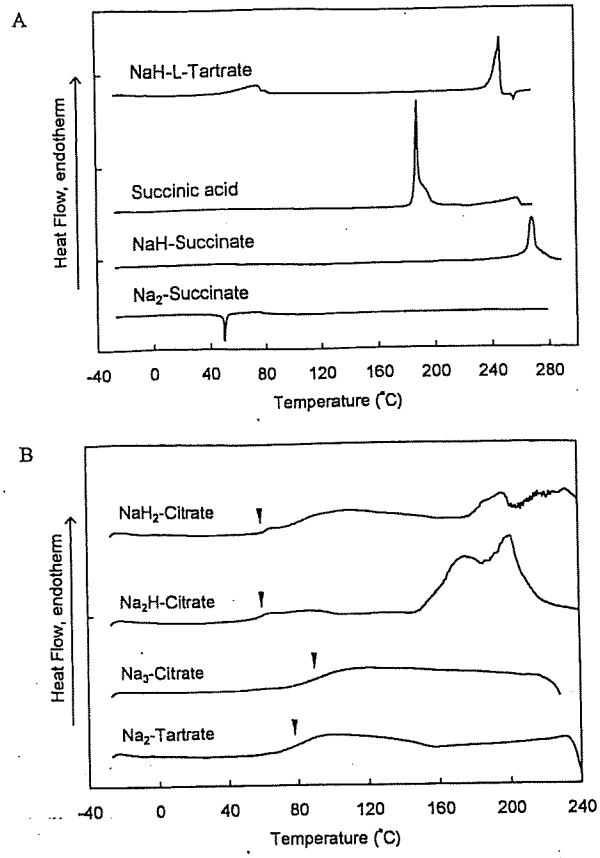

Fig. 1. Thermograms of Freeze-Dried Excipients (0.5—1 mg, 50 mM in Initial Solutions) Scanned from −30 °C at 5 °C/min

The solids presenting crystallization or melting peaks (A) and glass transitions (B) are shown at different heat flow scales. Arrowheads denote glass transitions of the freeze-dried solids (T_g).

(50 mM) showed endotherm peaks that indicate melting of the crystalline moiety (Fig. 1A). A crystallization exotherm at approximately 50 °C indicated the existence of an amorphous region in the freeze-dried disodium succinate solid. Frozen citric acid and L-tartaric acid solutions collapsed during the primary drying process, presumably because their T_g's were lower than the product temperature. Some diffraction peaks in powder X-ray diffraction patterns suggested partial crystallization of succinic acid and some salts (monosodium L-tartrate, disodium succinate) lyophilized in the absence of the protein (Fig. 2, some data not shown). Other organic acid salts formed glass-state amorphous solids during freeze-drying (Fig. 1B).

Co-lyophilization of the excipients (50 mM) with BSA (10 mg/ml) resulted in cylindrical cake-structure solids. Powder X-ray diffraction (XRD) analysis of the freeze-dried solids showed halo patterns that indicate largely amorphous components (Fig. 2). Most of the freeze-dried solids showed glass transitions at temperatures close to or much higher than room temperature in the thermal analysis (Table 1). The absence of a crystal melting peak in the heating scan (*e.g.*, monosodium citrate: 217 °C) also indicated the limited excipient crystallinity in the co-lyophilized solids. Karl–Fischer titrimetry indicated a relatively high residual water content in the freeze-dried solids (Table 1). The high protein mass ratio was one likely reason for the high residual water content in the solids freeze-dried without the organic acid salts.

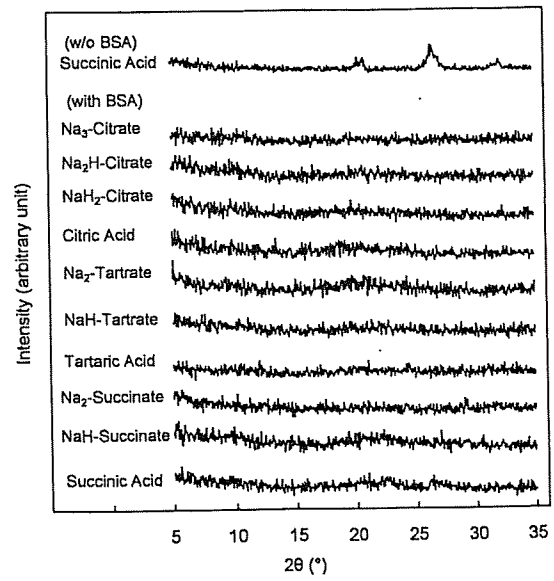

Fig. 2. Powder X-Ray Diffraction (XRD) Patterns of Excipients (50 mM) Freeze-Dried with or without BSA (10 mg/ml) and Corresponding Buffer Salts (1.5 mM)

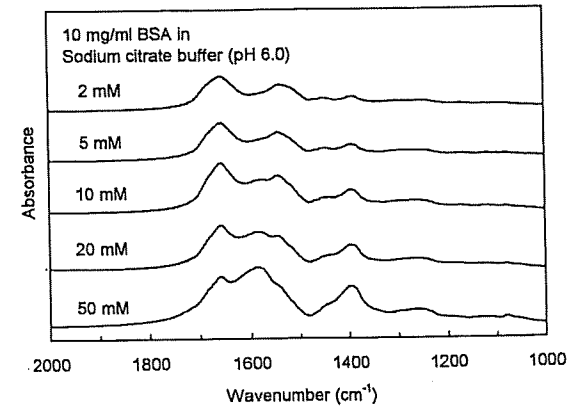

Fig. 3. FT-IR Spectra of BSA Freeze-Dried from Solutions Containing the Protein (10 mg/ml) and Various Concentrations (1.5—50 mM) of Sodium Citrate Buffer (pH 6.0)

FT-IR analysis was performed to elucidate the effect of buffer salts on the lyophilization-induced protein conformation change.[2,24,25] The following experiments were performed at certain (2—50 mM) buffer salt concentrations because of their overlapping absorbance in the co-lyophilized protein amide I band region (1600—1700 cm^{-1}) (Fig. 3). Figure 4 shows area-normalized second-derivative amide I spectra of BSA in solids freeze-dried from four buffer systems (20 mM, sodium phosphate, sodium citrate, sodium L-tartrate, sodium succinate, pH 6.0). A spectrum of the protein in its initial aqueous solution (10 mg/ml, 20 mM sodium citrate buffer, pH 6.0) was also included for comparison. The protein showed practically identical spectra in the four buffer solutions studied (Fig. 5). Freeze-drying of the protein from the buffer systems resulted in a varied extent of the lyophilization-induced structural perturbation as observed in the broad amide I spectra and reduced α-helix band (1656 cm^{-1}) intensity.[2,24,28—30] Larger structural changes were suggested in freeze-drying of the protein from sodium phosphate and sodium succinate buffer solutions.

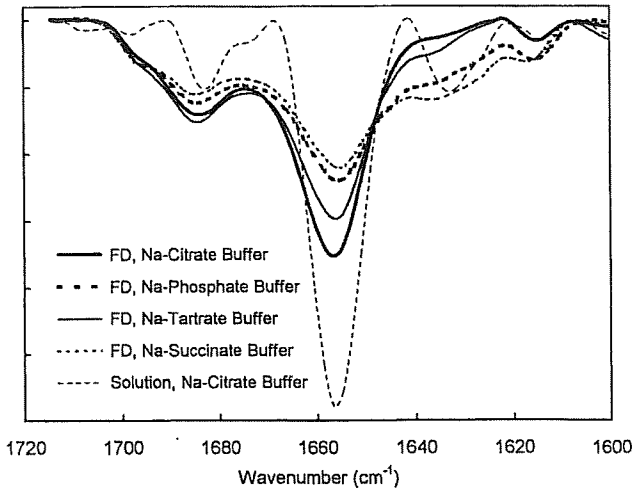

Fig. 4. Area-Normalized Second-Derivative Amide I Spectra of BSA Freeze-Dried from Solutions Containing the Protein (10 mg/ml) in Various Buffer Systems (20 mM, pH 6.0)

Fine dotted line denotes second-derivative spectra of BSA in the aqueous sodium phosphate buffer solution.

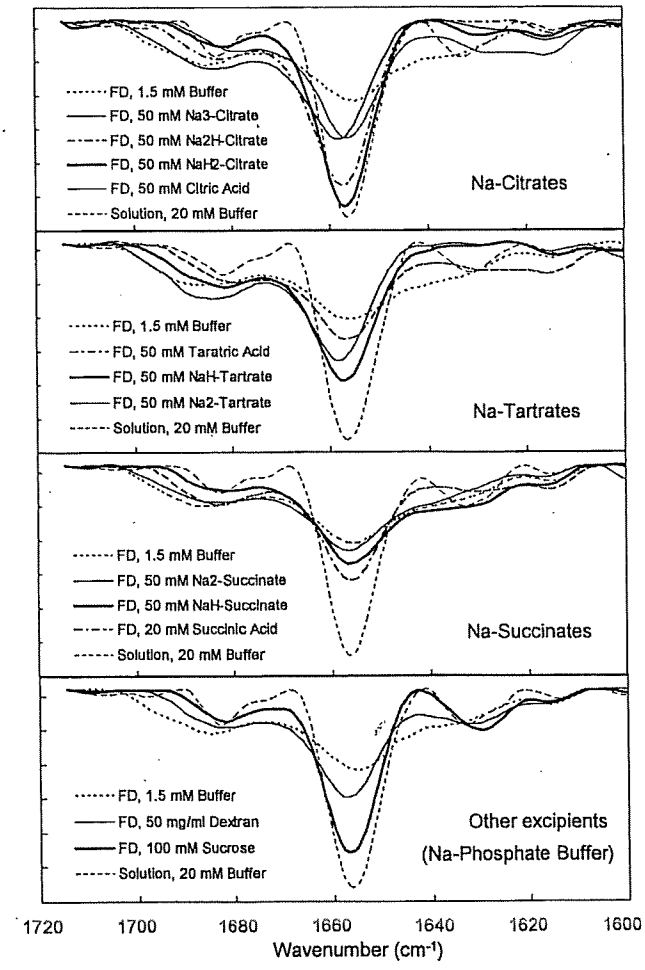

Fig. 5. Area-Normalized Second-Derivative Amide I Spectra of BSA Freeze-Dried from Aqueous Solutions Containing the Protein (10 mg/ml), Buffer Salts (1.5 mM), and Excipients (50 mM)

Fine dotted line denotes second-derivative spectra of BSA in the corresponding buffer solutions.

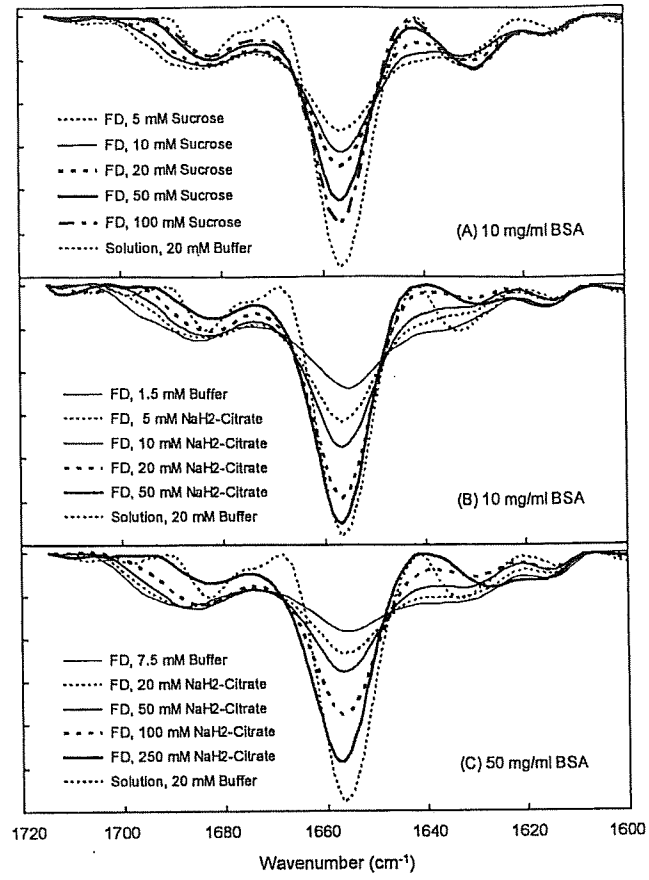

Fig. 6. Effect of Co-solutes on the Area-Normalized Second-Derivative Amide I Spectra of BSA Lyophilized at Different Concentrations (A, B: 10 mg/ml, C: 50 mg/ml).

Figure 5 shows area-normalized second-derivative amide I spectra of BSA freeze-dried with the organic acids and their salts (50 mM). Spectra of the protein in the corresponding buffer solutions (20 mM, pH 6.0) are also included. Freeze-drying of BSA (10 mg/ml) with the low concentration buffer components (1.5 mM) induced similar substantial structural changes. Monosodium citrate (50 mM) was most effective at retaining the large α-helix band that characterized the native protein structure upon freeze-drying. The spectra of BSA lyophilized at different concentrations (10, 50 mg/ml, Fig. 6) suggested the structure stabilized by monosodium citrate, which effect depended roughly on the salt/protein mass ratios. The α-helix band intensity reached a plateau at the salt concentrations (20—50 mM) lower than that of sucrose. Further addition of the salt induced a broader α-helix band presumably because of the overlapping absorbance (data not shown).

Other salts showed varied effects on the freeze-dried protein structures (Fig. 5). Disodium citrate and monosodium L-tartrate allowed BSA to retain its secondary structure to a lesser extent upon freeze-drying, compared to monosodium citrate. Trisodium citrate and citric acid were less effective at protecting the protein structure. Other organic acids and their salts showed a limited ability to protect the native protein conformation upon freeze-drying. The effect of succinic acid was studied at a lower (20 mM) concentration because of the large overlapping absorbance in the amide I region. Insuffi-

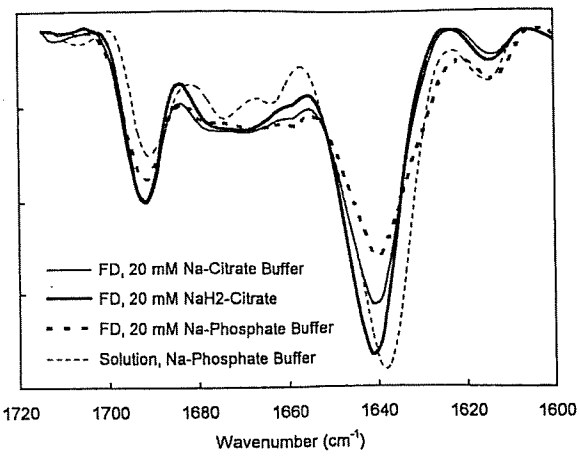

Fig. 7. Area-Normalized Second-Derivative Amide I Spectra of Immunoglobulin G in an Aqueous Buffer Solution (10 mg/ml) and Freeze-Dried Solids

The initial monosodium citrate solution (20 mM) also contained a lower (10 mM) concentration of sodium citrate buffer salts.

cient intermolecular interaction with co-lyophilized protein due to steric hindrance should explain the lower structure-stabilizing effect of dextran 10.2k compared to sucrose.[31] No apparent relationship between the structure-stabilizing effect and the glass transition temperatures (T_g) or residual water content of the freeze-dried solid (Table 1) was observed.

Second-derivative amide I spectra of bovine IgG showed predominant intramolecular (1637 cm^{-1}) and intermolecular (1692—1695 cm^{-1}) β-sheet bands (Fig. 7). The reduced intramolecular β-sheet band intensity indicated that IgG freeze-dried from sodium phosphate buffer (20 mM, pH 6.0) had a partially altered structure. Monosodium citrate (50 mM) allowed the IgG to retain the intramolecular β-sheet band upon freeze-drying. Retention of the predominant bands at different wavenumbers strongly suggested the effect of salt to stabilize native protein conformation rather than an artifact induced by the overlapping absorption.

Discussion

The results indicate that some organic acid salts form glass-state amorphous solids that protect proteins from structural change during freeze-drying. The carboxylic acids and their sodium salts showed varied physical properties in the frozen solutions and their dried solids.[4] A network of rigid carboxyl/carboxylate interaction and hydrogen bonds should explain the high glass transition temperature of the lyophilized amorphous sodium citrate solids.[32,33] Our previous study also showed contribution of rigid molecular interactions to form glass-state solids by co-lyophilization of citric acid an L-arginine.[34] Many protein solutions have their T_g' at temperatures (approx. -10 °C) higher than those of smaller molecules.[27] The addition of proteins should reduce the mobility of other solute molecules in the freeze-concentrated phase, and thus prevent eutectic solute crystallization.

Freeze-drying of the protein in the sodium phosphate (20 mM) or lower concentrations of the carboxylic acid buffers (1.5 mM) perturbed their secondary structure. The structurally perturbed molecules usually return to their native structure upon re-hydration, whereas misfolding and/or binding between exposed hydrophobic regions are major causes of the lyophilization-induced protein aggregation. The structurally altered protein molecules are also prone to chemical degradation during storage.[1,2,24] Some glass-forming organic acid sodium salts (*e.g.*, sodium citrates) maintained the native secondary structure of co-lyophilized BSA and IgG. Such structural stabilization would explain the higher residual activity of proteins after freeze-drying from certain buffer systems.[12—16]

The organic acids should protect proteins through several mechanisms in the different physical states prior to and during the freeze-drying process. The fatty acid-poor BSA is most resistant to heat denaturation in weakly acidic to neutral (pH 5—7) solutions.[35] Freeze-drying of the protein in the region (pH 6.0) resulted in varied secondary structures depending on the buffer systems. Observed structural stabilization at certain salt/protein concentration ratios indicated the contribution of the direct interactions. It is highly plausible that the effective buffer salts provide proteins hydrogen bonds that substitute for those of the surrounding water molecules inevitable to retain the conformation. In addition, the lower effective concentration of monosodium citrate compared to sucrose suggested the contribution of electrostatic (ion–ion, ion–dipole) interactions between the salt anion (hydroxycarboxylate ion) and basic amino acid residues on protein surfaces for the structural stabilization.[17,36,37] The high T_g of the dried solids indicated mixing of the protein and salts required for the interaction. The topic of protein-stabilizing molecular interactions in the dried states, including the effect of differently ionized functional groups, will require further study for elucidation. The limited mobility of the surrounding molecules should prevent chemical degradation of the protein in glass-state solids. Similar structural (thermodynamic) and chemical (kinetic) stabilization of embedded proteins has been reported in disaccharides.[22,23] Some of the buffer components should also protect proteins from cold denaturation in the aqueous solutions and in the frozen solutions. The citrate^{3-} and L-tartrate^{2-} ions are 'kosmotropic' anions that thermodynamically stabilize native protein structures by being preferentially excluded from the immediate surface of the protein molecules.[16,17,22,38—41] In other words, the proteins are preferentially hydrated in the solute solutions.

The difference in the structure and physical properties would explain the varied protein-stabilizing effect of the organic acid salts through the above-mentioned mechanisms. Solution pH and anion structure are major factors that determine the thermal stability of proteins in aqueous carboxylic acid salt solutions.[17] Some di- and tricarboxylic acid salts protect proteins from thermal denaturation. The number of carboxyl and hydroxyl groups should is also likely to be important in protecting the secondary structure of BSA through the water-substituting hydrogen bonds and electrostatic interactions against the dehydration stress. The limited structure-stabilizing effect of succinic acid and its salts during freeze-drying, in spite of their apparent effect to improve the thermal stability of proteins in aqueous solutions, suggests that the hydroxyl group makes a large contribution to the structural stabilization against dehydration stresses. Possible salt crystallization at a higher salt/protein concentration ratio should further reduce the stabilizing interactions between them. Monosodium citrate should satisfy various requirements (*e.g.*, sufficient functional groups, appropriate ionized

states, propensity to form glass-state amorphous solids) for protein-stabilizing interactions in the dried states.

Our results emphasize the importance of choosing an appropriate buffer system when developing freeze-dried protein formulations. Salts that have a higher propensity for crystallization should be avoided especially at lower excipient/protein concentration ratios. Significant stabilizing effects of some organic acid salts are applicable to the design of sugar-free formulations. Some buffer components also raise the glass transition temperature of co-lyophilized disaccharide solids.[42,43] The retention of protein structural integrity in the amorphous salt solids would also be relevant to other applications of proteins in ionic environments, including enzyme reactions in ionic liquids (RTMS: room temperature molten salts).[44—46] Careful optimization of ingredients based on the physical and chemical properties of the excipients should ensure the optimal processing and storage stability of protein formulations.

Acknowledgements This work was supported in part by the Japan Health Sciences Foundation (KHB1006).

References

1) Chang B. S., Beauvais R. M., Dong A., Carpenter J. F., *Arch. Biochem. Biophys.*, **331**, 249—258 (1996).
2) Prestrelski S. J., Tedeschi N., Arakawa T., Carpenter J. F., *Biophys. J.*, **65**, 661—671 (1993).
3) Hermeling S., Crommelin D. J., Schellekens H., Jiskoot W., *Pharm. Res.*, **21**, 897—903 (2004).
4) Shalaev E. Y., Johnson-Elton T. D., Chang L., Pikal M. J., *Pharm. Res.*, **19**, 195—201 (2002).
5) MacKenzie A. P., *Bull. Parenter. Drug Assoc.*, **20**, 101—130 (1966).
6) Akers M. J., Vasudevan V., Stickelmeyer M., *Pharm. Biotechnol.*, **14**, 47—127 (2002).
7) Williams-Smith D. L., Bray R. C., Barber M. J., Tsopanakis A. D., Vincent S. P., *Biochem. J.*, **167**, 593—600 (1977).
8) Murase N., Franks F., *Biophys. Chem.*, **34**, 293—300 (1989).
9) Sarciaux J. M., Mansour S., Hageman M. J., Nail S. L., *J. Pharm. Sci.*, **88**, 1354—1361 (1999).
10) Pikal-Cleland K. A., Rodriguez-Hornedo N., Amidon G. L., Carpenter J. F., *Arch. Biochem. Biophys.*, **384**, 398—406 (2000).
11) van den Berg L., Rose D., *Arch. Biochem. Biophys.*, **81**, 319—329 (1959).
12) Hynes H. E., Owen C. A. J., Bowie E. J., Thompson J. H. J., *Blood*, **34**, 601—609 (1969).
13) Osterberg T., Fatouros A., Mikaelsson M., *Pharm. Res.*, **14**, 892—898 (1997).
14) Chang B. S., Reeder G., Carpenter J. F., *Pharm. Res.*, **13**, 243—249 (1996).
15) Labrude P., Vigneron C., *J. Pharm. Pharmacol.*, **32**, 305—307 (1980).
16) Busby T. F., Atha D. H., Ingham K. C., *J. Biol. Chem.*, **256**, 12140—12147 (1981).
17) Kaushik J. K., Bhat R., *Protein Sci.*, **8**, 222—233 (1999).
18) Li J., Chatterjee K., Medek A., Shalaev E., Zografi G., *J. Pharm. Sci.*, **93**, 697—712 (2004).
19) Arakawa T., Timasheff S. N., *Biochemistry*, **21**, 6536—6544 (1982).
20) Carpenter J. F., Crowe J. H., *Biochemistry*, **28**, 3916—3922 (1989).
21) Izutsu K., Yoshioka S., Terao T., *Pharm. Res.*, **10**, 1232—1237 (1993).
22) Carpenter J. F., Prestrelski S. J., Arakawa T., *Arch. Biochem. Biophys.*, **303**, 456—464 (1993).
23) Franks F., *Dev. Biol. Stand.*, **74**, 9—18 (1992).
24) Dong A., Prestrelski S. J., Allison S. D., Carpenter J. F., *J. Pharm. Sci.*, **84**, 415—424 (1995).
25) Susi H., Byler D. M., *Biochem. Biophys. Res. Commun.*, **115**, 391—397 (1983).
26) Kendrick B. S., Dong A., Allison S. D., Manning M. C., Carpenter J. F., *J. Pharm. Sci.*, **85**, 155—158 (1996).
27) Chang B. S., Randall C., *Cryobiology*, **29**, 632—656 (1992).
28) Carter D. C., Ho J. X., *Adv. Protein Chem.*, **45**, 153—203 (1994).
29) Murayama K., Tomida M., *Biochemistry*, **43**, 11526—11532 (2004).
30) Luthra S., Kalonia D. S., Pikal M. J., *J. Pharm. Sci.*, **96**, 2910—2921 (2007).
31) Kreilgaard L., Frokjaer S., Flink J. M., Randolph T. W., Carpenter J. F., *J. Pharm. Sci.*, **88**, 281—290 (1999).
32) Kadoya S., Izutsu K., Yonemochi E., Terada K., Yomota C., Kawanishi T., *Chem. Pharm. Bull.*, **56**, 821—826 (2008).
33) Inabe T., *J. Mater. Chem.*, **15**, 1317—1328 (2005).
34) Izutsu K., Kadoya S., Yomota C., Kawanishi T., Yonemochi E., Terada K., *Chem. Pharm. Bull.*, **57**, 43—48 (2009).
35) Gumpen S., Hegg P. O., Martens H., *Biochim. Biophys. Acta*, **574**, 189—196 (1979).
36) Tian F., Middaugh C. R., Offerdahl T., Munson E., Sane S., Rytting J. H., *Int. J. Pharm.*, **335**, 20—31 (2007).
37) Izutsu K., Fujimaki Y., Kuwabara A., Aoyagi N., *Int. J. Pharm.*, **301**, 161—169 (2005).
38) Arakawa T., Timasheff S., *Biochemistry*, **23**, 5912—5923 (1984).
39) Hofmeister F., *Arch. Exp. Pathol. Pharmakol.* (Leipzig), **24**, 247—260 (1888).
40) Jensen W. A., Armstrong J. M., Giorgio J. D., Hearn M. T., *Biochim. Biophys. Acta*, **1296**, 23—34 (1996).
41) Ru M. T., Hirokane S. Y., Lo. A. S., Dordick J. S., Reimer J. A., Clark D. S., *J. Am. Chem. Soc.*, **122**, 1565—1571 (2000).
42) Ohtake S., Schebor C., Palecek S. P., de Pablo J. J., *Pharm. Res.*, **21**, 1615—1621 (2004).
43) Kets E. P., IJpelaar P. J., Hoekstra F. A., Vromans H., *Cryobiology*, **48**, 46—54 (2004).
44) Fujita K., MacFarlane D. R., Forsyth M., *Chem. Commun.* (Camb.), **2005**, 4804—4806 (2005).
45) van Rantwijk F., Madeira L. R., Sheldon R. A., *Trends Biotechnol.*, **21**, 131—138 (2003).
46) Ohno H., *Bull. Chem. Soc. Jpn.*, **79**, 1665—1680 (2006).

バイオ後続品とは　ー開発状況と規制についてー

川西　徹[1]

要旨：　国際的にバイオ医薬品後発品（バイオ後続品）の開発が活発化し、規制の枠組みの構築が行われつつある。バイオ後続品は後発医薬品と異なり、先発バイオ医薬品との同等・同質性を示すために、品質特性評価データに加えて、通常非臨床・臨床試験データが必要とされる。したがって従来の後発医薬品と異なる規制の枠組みが必要である。欧州はいち早く規制体制を確立し、既に約10の製品が承認されている。我が国においても開発が活発化しており、承認された製品はまだないが、バイオ後続品ガイドラインが近々に公表される予定であり、広く臨床で使用されるようになると思われる。

1．今なぜバイオ医薬品後発品が注目されるのか？

バイオ医薬品は1982年に米国でヒトインスリンを第一号として認可され、その後様々な製品が開発され、世界各国で認可、臨床で広く使用されている。現在、バイオ医薬品の後発品が話題となっている第一の理由は、これらの製品の中で2001年から特許の期限を迎える製品があり、その数は年々増えており、後発品開発の対象となったことである[1-2)]。タンパク質性医薬品の場合、分子量の小さい化学合成薬品のように構造が判っていれば容易に製造できるという訳ではない。しかしながら、欧米の後発品メーカー、あるいはアジア諸国の製薬企業を中心に、バイオ医薬品の後発品開発の機運が高まっている。第二の理由としては、先進国における医療費高騰があげられる。先進国においては、高齢化も相まって医療費の高騰が社会経済的に大きな負担となっており、医療費の中で大きな割合を占める薬剤費の節約は医療費削減に向けた大きな目標となっている。一方発展途上国においては、多くのバイオ医薬品は高額ゆえに患者さんのもとに届きにくいという事情もある。このような背景の中、欧米では既にいくつかの製品が認可をうけており、さらにアジア諸国の中には、既に多くの製品が認可されている国がある。一方、我が国においても、特許が切れた製品が増えるにつれ、開発の機運が高まっており、既に承認申請されているものもあり、開発途上にある製品は少なくない。

2．バイオ医薬品の後発品は「バイオ後続品」

化学合成医薬品の場合、独占的販売期間（特許期間や再審査期間）を過ぎると先発医薬品企業以外の製薬企業が、後発医薬品として製品開発を行い、安い価格で販売する制度が社会的に受け入れられている。後発医薬品の条件としては、(1)先発品と有効成分が同一であり、(2)先発品と同一用法・用量の投与で、同一の効能・効果を示す、ということである。化学合成医薬品の後発品を承認申請するにあたっては、開発企業は (1)有効成分の同一性、

[1] 国立医薬品食品衛生研究所薬品部　部長（かわにし　とおる）

(2)不純物の安全性、(3)製剤の安定性、(4)製剤の生物学的同等性、さらには(5)製造の一定性に関する資料の提出を求められ、評価をうける。

バイオ医薬品の後発品の評価も視点は同様である。しかし、有効成分の特性の違い、あるいは分析手法の限界等により、評価の現実に大きな違いがある。すなわち

(1) 有効成分の同一性： タンパク質性医薬品では一次構造（アミノ酸配列）の同一性を示すことは容易であるが、高次構造の同一性の確認は困難である。そこで生物活性が重要な指標となるが、臨床効果に直結するヒト型タンパク質の生物活性の測定は必ずしも容易ではなく、またその結果が同一性を保証するものでもない。さらに、糖タンパク質などのように翻訳後修飾により分子多様性を示す有効成分については、同一性の定義すら困難である。したがって多くの製品においては「有効成分の同一性」評価ではなく、「有効成分の類似性」の評価が目標となる。

(2) 不純物の安全性評価： 化学合成医薬品においても製品が異なると不純物パターンは異なる。しかし化学合成医薬品においては、ICH 不純物ガイドライン[3]に準じた基準で安全性評価は可能である。一方多くのバイオ医薬品においては、不純物の生物作用も種特異性を示す場合が高く、安全性の最終的な確認は臨床試験データによるところが大きい。

(3) 製剤の安定性： 一般に化学合成医薬品では、加速試験（実保存条件より高温、高湿での試験）データで保存条件での安定性の予測が可能である。しかし、バイオ医薬品では実保存時間、実保存条件での評価が必要である。

(4) 製剤の生物学的同等性： 多くの化学合成医薬品では作用部位での有効成分の濃度の同等性（循環血中に吸収されて作用する医薬品では血中濃度の同等性）を示すことにより生物学的同等とされる。しかしバイオ医薬品においては、同等性は作用部位での濃度の同等性に加えて、生物活性の同等性に依存する。さらにタンパク質性医薬品では体内動態の定量的解析をするには技術的な制約が多い。

(5) 製造の一定性評価： バイオ医薬品の基本原則は化学合成医薬品と違いはないものの、製造にブラックボックスともいえる生物材料を用い、さらに有効成分は不安定なものが多く、一定性の評価にも独特の視点が必要である。

以上の理由により、バイオ医薬品の後発品を承認する上では、品質特性の比較データに加え、非臨床試験、臨床試験データを適宜組み合わせて評価することが妥当と考えられている。したがって、規制上でも「後発医薬品」とは別のカテゴリーを設ける方策がとられている。即ち、下記に詳述するように、欧州では「バイオシミラー（Biosimilar products）」、米国では「後続品（Follow-on products）」、カナダでは「後続参入製品（Subsequent-entry products）」などと称され、各国の規制制度に応じた枠組みの規制が行われている。我が国においては、新有効性成分医薬品とも後発医薬品とも異なる、新しい承認申請区分が設けられ、「バイオ後続品」と呼ばれる予定である。そのため、本稿では総称としては「バイオ後続品」を用いる。

なお、欧米では後発医薬品は有効成分に対応する一般的名称で処方されることが多く「ジ

ェネリック医薬品」とも呼ばれることから、バイオ後続品を「バイオジェネリック」と称することがあるが、バイオ後続品は有効成分からいっても先発品と同一とはいえない製品が多く、この総称は適切ではない。

3．欧米におけるバイオ後続品の規制状況および開発

（3－1）欧州におけるバイオ後続品の承認申請の動き

欧州では、2003年ヒト成長ホルモン製剤（ジェノトロピン）の後続品としてオムニトロープがサンド社により簡易医薬品申請され、それと平行してバイオ後発品の承認審査における規制ルートの議論が開始された。その結果、欧州におけるヒト医薬品の申請に関する法律（Directive 2001/83/EC）中の後発医薬品（Article 10(1)(a)(iii)）の承認申請のために必要とされる評価資料では十分でないとし、2003年6月に当該法律を改正し、SBMP(Similar Biological Medicinal Product (略してBiosimilar)) という承認申請カテゴリーを新たに追加した（Directive 2003/63/EC）。SBMPでは品質特性における同等・同質評価に加え、さらに非臨床試験および臨床試験評価が必要であり、それらの試験で必要とされるデータの程度はケースバイケースである。即ち、SBMPの承認申請にあたっては、新薬と同様の品質特性データ、略式非臨床試験・臨床試験のデータに加えて、先発バイオ医薬品との品質特性に関する同等性／同一性評価データ、さらには多くの製品で同等性／同質性を明らかにするための非臨床、臨床評価データが必要となる。また、これら申請データの作成に関して参照すべきガイドラインとして、欧州医薬品審査庁（EMEA）の科学委員会CHMPは３つの基本ガイドライン（総論、品質、非臨床・臨床）に加えて、非臨床・臨床評価ガイドラインの補遺として先発品の有効成分に応じた４つのガイドライン（ヒトインスリン、成長ホルモン、エリスロポエチン、GCSF）、さらに２つの非臨床・臨床評価ガイドラインドラフト（インターフェロン-α、低分子量ヘパリン）を公表している。

このように、欧州では世界に先駆けてバイオ後続品の規制システムを整備し、Omnitropeを第一号として、既に２つのソマトロピン後続品、５つのエポエチンα後続品、４つのフィルグラスチム後続品が承認されている。（表２参照）

（3－2）米国におけるバイオ後続品の規制状況及び開発

米国におけるバイオ後続品の規制は複雑な状況にある。米国でもオムニトロープが2003年7月にFDAに承認申請され、審査されたが、承認の可否について決定するには至らなかった旨、申請者に告げられた。その理由としては、米国においてバイオ後続品を認可する上での、規制上の枠組みが明確でないことが指摘されている。この経過を不服として、サンド社は2005年9月にFDAを提訴し、その結果、裁判所より、FDAに結論を出すよう裁定が下され、FDAは2006年にオムニトロープを承認した。

米国でバイオ後続品の受入が混乱する理由としては、米国の医薬品規制システムにおいて、バイオ後続品を承認する規制制度が不十分であることにある。米国ではバイオ医薬品

は公衆衛生サービス法と食品医薬品化粧品法の二つによって規制されており、前者には簡略非臨床・臨床データにより承認するシステムはない。一方後者には化学合成医薬品の後発医薬品を承認する枠組みはあるものの、略式の非臨床・臨床データによりバイオ後続品を承認する枠組みが整備されていない。それでも後者には他製品の非臨床・臨床試験データを利用して申請できる簡略申請システムがあり、上記オムニトロープもこのルートで承認された。またオムニトロープ以外にも、同様のルートで既に承認されているバイオ製品もある（表１参照）。しかし、バイオ後続品を本格的に承認する法的ルートとしては不十分であり、米国議会で前者のルートで簡略申請を可能にする改正法案が審議されているようである。しかし、先発企業と後続企業との利害の対立により法案成立には時間がかかっている[4]。

このような事情により、米国FDAによるバイオ後続品の本格的なガイドライン作成は遅れているが、Woodcockによる米国下院での証言[5]にもみられるように、今後対策を急ぐ気配がみえている。

（３－３）世界保健機関（WHO）におけるガイドライン作成

バイオ後続品の必要性は先進諸国ばかりでなく発展途上の国においても叫ばれている。そこでWHOでは、2007年4月からバイオ後続品ガイドライン作成が開始された[6]。世界的にみると、先発バイオ製品が国内で開発されておらず、先発製品との比較データなしに既にバイオ後続品が承認されている国もある。したがって、WHOガイドラインドラフトは複雑なものとなっており、日本を含めた欧米のように、国内の既承認先発バイオ医薬品との同等性・同質性データを必須とする方策に加え、先発バイオ医薬品の文献データ等との比較のみで可とするという方策をも認めるガイドラインとなる可能性がある。

（３－４）我が国におけるバイオ後続品の規制および開発状況

上記のような状況の中、我が国おいてもバイオ後続品の承認申請がなされており、バイオ後続品ガイドラインも2009年前半には公表される予定である。我が国におけるバイオ後続品評価の考え方は、基本的には欧州と同様である。即ち、開発企業は独自に製造方法を確立した上で、先発企業と同様のレベルの品質特性データ、さらには既承認先発バイオ医薬品との同等性・同質性評価データを提出、承認審査をうけることが必要とされる。その際、通常は品質特性の比較に加えて、非臨床・臨床試験による比較データが必要となる。さらに、特に安全性に関わる市販後調査は重要である。後発医薬品とは異なり、先発バイオ医薬品とバイオ後続品を、一連の治療期間内に代替または混用することは基本的には避ける必要がある旨明記される予定である。

４．バイオ後続品の今後

バイオ後続品の開発対象は、現在のところ、成長ホルモン、エリスロポエチン、GCSF、

ヒトインスリン等に限られている。しかしながら、今後インターフェロン、モノクローナル抗体[7]等についても開発が活発に試みられるようである。ただし、簡略化されてはいるものの、ある程度の臨床データが必要であることもあり、開発コストが後発医薬品のように安くなるということはない。実際、承認が先行している欧州においても、バイオ後続品が急速に先発医薬品に置き換わるような状況にはなっていないようである。とはいえ、長期的には確実に普及し、バイオ医薬品の中で重要な位置を占めることになると思われる。

文献

1) Walsh G: Biopharmaceutical benchmarks-2003, *Nature Biotech*, **21**, 865-870 (2003)
2) Walsh,G: Biopharmaceutical benchmarks-2006, *Nature Biotech*, **24**, 769-774 (2006)
3) Inpurities in New Drug Products: ICH Harmonized Tripartite Guideline (http://www.pmda.go.jp/ich/q/q3br2_06_7_3e.pdf)
4) Grabowski H: Follow-on biologicals: data exclusivity and the balance between innovation and competition, *Nature Review Drug discovery*, **7**, 479-488 (2008)
5) Woodcock J: Follow-on Protein Products" Statement before the Committee on Oversight and Government Reform, U.S. House of Representatives, 26 March 2007. FDA web site [on line], http://www.fda.gov/ola/2007/protein32607.html (2007)
6) Meeting Reports: WHO Informal consultation on Regulatory Evaluation of Therapeutic Biological Products (http://www.who.int/biologicals/areas/biological_therapeutics/Final%20Biosimilar%20meeting%20Report%20for%20web%2013%20September%202007.pdf)
7) Schneider CK et al.: Toward biosimilar monoclonal antibodies, *Nature Biotech*, **26**, 985-990 (2008)

表1　　欧米で既承認のバイオ後続品

国際一般名称）	先行品	後続品	開発企業	EU	FDA
Somatropin	ジェノトロピン	オムニトロープ	Sandoz	2006	2006
Somatropin	ヒューマトロープ	バルトロピン	BioPartners, LG Life	2006	2007
Epoetin alfa	エプレックス/エリポ	ビノクリット	Sandoz	2007	–
Epoetin alfa	エプレックス/エリポ	エポエチンアルファ　ヘキサル	Hexal Biotech	2007	–
Epoetin alfa	エプレックス/エリポ	アブセアメド	Medicine Arzneimittel	2007	–
Epoetin zeta	エプレックス/エリポ	シラポ	Stada Arzneimittel	2008	–
Epoetin zeta	エプレックス/エリポ	レタクリット	Hospira	2008	–
Filgrastim	ノイポジェン	テバグリスチム	Teva Generics	2008	–
Filgrastim	ノイポジェン	ラチオグリスチム	Rationpharm	2008	–
Filgrastim	ノイポジェン	ビオグラスチム	CT Arzneimittel	2008	–
Filgrastim	ノイポジェン	フィログラスチムラチオファム	Ratiopharm	2008	–

有効成分	後続品	開発企業	EU	FDA
グルカゴン(遺伝子組換え)	グルカゴン	Novo Nordisk	–	1998
ヒアルロニダーゼ	アンファダーゼ	Amphastar Pharm	–	2004
サケカルシトニン(遺伝子組換え)	フォルチカル	Upsher Smith	–	2005
ヒアルロニダーゼ	ハイダーゼ	Primapharm	–	2005
ヒトヒアルロニダーゼ(遺伝子組換え)	ハイレネックス	Halozyme Therap	–	2005

バイオ後続品の評価

川西 徹
Toru KAWANISHI
国立医薬品食品衛生研究所薬品部長

1 はじめに

バイオ医薬品の後発品の開発が活発化している．背景としては独占的販売権が切れたバイオ医薬品が増えていることにあるが，化学合成医薬品の後発医薬品と同様の規制の枠組みで評価可能かどうか，議論がされている．そこで本稿では，欧米等の開発及び規制動向をまとめるとともに，我が国におけるこれら医薬品の評価の基本原則について考察した．

2 バイオ医薬品の後発品の登場

バイオ医薬品は1982年に米国においてヒトインスリンが初めて認可されて以来，数多くの製品が開発され，世界各国で臨床使用されており，標準的治療薬としての地位を得ている医薬品も少なくない．最近バイオジェネリックあるいはバイオシミラー等の名称で，これらバイオ医薬品の後発品が話題となることが多いが，その理由の第1は，バイオ医薬品の中で2001年から特許が切れる製品があり，その数は年々増えており後発品開発の対象となっていることである．[1,2] 第2の理由としては，先進国における医療費高騰があげられる．先進国においては，高齢化も相まって医療費の高騰が社会経済的に大きな負担となっており，医療費の中で大きな割合を占める薬剤費の節約は医療費削減に向けた大きな目標となっている．第3の理由としては多くのバイオ医薬品は高額ゆえに患者のもとに届きにくいという事情があり，開発コストの安い後発医薬品のシステムを活用し有用な医薬品資源を有効に活用しようという動きがある．このような背景のなか，欧米では既に幾つかの製品が認可をうけており，アジア諸国の中にも既に多くの製品が認可されている国がある．一方，我が国においても開発の機運は高まっており，既に承認申請されているものもあり，開発途上にある製品も少なくない．これらの製品については，下記に記すような理由により，欧米では後発医薬品とは別のカテゴリーで規制するという方向にあり，我が国では「バイオ後続品」という総称で規制をうけることとなった．そこで，本稿では以下「バイオ後続品」を用いることとする．

3 バイオ後続品の開発及び規制の状況

化学合成医薬品の場合，独占的販売期間(特許期間や再審査期間)を過ぎると先発医薬品企業以外の製薬企業が，特に開発コストのかかる非臨床・臨床試験については生物学的同等性試験以外の試験を必要としない後発医薬品として製品開発を行い，低価格で販売する制度が社会的に受け入れられている．しかしこの後発医薬品の規制システムは，バイオ後続品については不適当

ということが欧米の共通認識となっており，どのような規制体制をとるべきか議論されている．

1．欧州におけるバイオ後続品の開発及び規制の状況

欧州では，2003年ジェノトロピン(ヒト成長ホルモン製剤)のバイオ後続品としてオムニトロープがサンド社によって簡易医薬品申請された．その過程において，バイオ後続品の承認審査における規制ルートの議論が開始された．その結果，欧州におけるヒト医薬品の申請に関する法律(Directive 2001/83/EC)にある後発医薬品(Article 10(1)(a)(iii))の承認申請用評価資料では不十分として，2003年6月に当該法律を改正し，SBMP(Similar Biological Medicinal Product(略してバイオシミラー Biosimilar product))という承認申請カテゴリーを新たに追加した(Directive 2003/63/EC)．SBMPの承認申請にあたっては，新薬と同様の品質特性データ，略式非臨床試験・臨床試験のデータに加えて，先発バイオ医薬品との品質特性に関する同等性/同一性評価データ，さらには多くの製品で同等性/同質性を明らかにするための非臨床，臨床評価データが必要となった．その際参照すべきガイドラインとして，3つの基本ガイドライン(総論，品質評価，非臨床・臨床評価)に加えて，非臨床・臨床評価ガイドラインの補遺として先発品の有効成分に応じた4つのガイドライン(ヒトインスリン，成長ホルモン，エリスロポエチン，G-CSF)，さらに2つの非臨床・臨床評価ガイドライン補遺ドラフト(インターフェロン-α，低分子量ヘパリン)が，欧州医薬品審査庁(EMEA)の科学委員会CHMPによって作成，公表された．[3]

このように，欧州では世界に先駆けてバイオ後続品の規制システムを整備し，オムニトロープを第1号として，既に2つのソマトロピン後続品，5つのエポエチンα後続品，5つのフィルグラスチム後続品が承認されている(表1参照)．

2．米国におけるバイオ後続品の開発及び規制の状況

米国におけるバイオ後続品(米国ではFollow-on productと称している)の規制は複雑な状況にある．米国でも，オムニトロープが2003年7月にFDAに承認申請され審査されたが，FDAは申請内容に問題はないとしながら結論を示さなかった．この経過を不服として，サンド社は2005年9月にFDAを提訴し，その結果，裁判所よりFDAに結論を出すよう裁定が下され，FDAは2006年にオムニトロープを承認した．このように米国でバイオ後続品の受入れが混乱

表1　欧州連合及び米国FDAで認可されているバイオ後続品リスト[a]

国際一般的名称	先発品	後続品	開発企業	EU	FDA
Somatropin	ジェノトロピン	オムニトロープ	Sandoz	2006	2006
Somatropin	ヒューマトローブ	バルトロピン	BioPartners，LG Life	2006	2007
Epoetin alfa	エプレックス/エリポ	ビノクリット	Sandoz	2007	−
Epoetin alfa	エプレックス/エリポ	エポエチンアルファ　ヘキサル	Hexal Biotech	2007	−
Epoetin alfa	エプレックス/エリポ	アブセアメド	Medicine Arzneimittel	2007	−
Epoetin zeta	エプレックス/エリポ	シラポ	Stada Arzneimittel	2008	−
Epoetin zeta	エプレックス/エリポ	レタクリット	Hospira	2008	−
Filgrastim	ニューポジェン	テバグラスチム	Teva Generics	2008	−
Filgrastim	ニューポジェン	ラティオグラスチム	Rationpharm	2008	−
Filgrastim	ニューポジェン	ビオグラスチム	CT Arzneimittel	2008	−
Filgrastim	ニューポジェン	フィログラスチムラティオファム	Ratiopharm	2008	−
Filgrastim	ニューポジェン	ザルジオ	Sandoz	2009	−

a)石井博士，山口博士(国立医薬品食品衛生研究所生物薬品部)からの情報提供により作成．